

Deviation from the Inverse-Thickness Relation in Gas-Metal Permeation

J. R. PHILLIPS and B. F. DODGE

Yale University, New Haven, Connecticut

The permeation rate of hydrogen through cylindrical membranes of type 321 stainless steel was determined under a wide range of conditions. The pressure was varied from 0.1 to 30.0 atm. and the temperature from 300° to 800°C. Four permeation membranes were used with wall thicknesses of 0.0252, 0.1003, 0.1011, and 0.2475 cm.

The permeation rate was found to deviate from the square-root-of-pressure and inverse-thickness relations predicted by the Richardson equation. Slow surface reactions are considered to be the cause of the observed deviations. The permeation data were correlated by a semiempirical interfacial resistance model.

Permeation rates were observed to increase with time of membrane exposure to hydrogen. It is believed this resulted from changing surface activity.

The subject of the flow of gases into and through metals is a broad one with many facets. However it has been the generally harmful effect of certain gases on the mechanical properties of metals that has fostered a desire to understand the fundamental mechanisms by which gases permeate metals.

The present study was designed to shed light on the relative importance of kinetic steps at the gas-metal interface and diffusion through the metal lattice as rate-controlling factors in the permeation process.

THEORY

Basic Permeation and Diffusion Relations

Throughout this discussion it is necessary to keep in mind the distinction between the terms *permeation* and *diffusion* as they apply to gas flow in metals. Permeation may be defined as the process of molecules passing from one gas phase through a metal barrier and into a second gas phase, while diffusion is concerned with the movement of gas atoms within the metal only. The diffusion step is the rate-controlling one in most cases, but in others it may have a negligible effect on the overall permeation rate.

The movement of a diffusing component within a metal lattice is described by Fick's first law. For the case of gas atoms diffusing radially in a thin-wall hollow cylinder of length L , radii r_2 and r_1 ($r_2 > r > r_1$), and concentration maintained at c_1 at r_1 and c_2 at r_2 ($c_1 > c_2$) for all time, Fick's first law can be developed to the following expression for the steady state rate of diffusion:

$$R = \frac{2\pi r_a L D (c_1 - c_2)}{(r_2 - r_1)} \quad (1)$$

where the system is at some constant temperature T , and D is assumed to be independent of concentration.

A primary difficulty in studying the flow of a gas through a metal is that the values of c_1 and c_2 may not readily be determined directly and in general must be inferred from some assumed relation to the applied pressure. For instance in a hydrogen-steel system it is an established fact (18) that the equilibrium between hydrogen gas and hydrogen dissolved in the metal (at constant temperature) may be expressed by Sieverts' law:

$$c = Kp^{1/2} \quad (2)$$

It is from this experimental observation that the presence of hydrogen in atomic form within the metal has been deduced.

If the concentration of hydrogen just inside the surface of a hollow metal cylinder is in equilibrium with the hydrogen pressure applied to the surface, Equations (1) and (2) may be combined to yield

$$R = \frac{2\pi r_a L D K (p_1^{1/2} - p_2^{1/2})}{(r_2 - r_1)} \quad (3)$$

Although it applies to a special case of diffusion, Equation (3) is really a permeation equation rather than a diffusion equation, since gas pressure is now considered to be the driving force involved.

It is well established (3) that at least in the simplest case both D and K vary exponentially with temperature and may be expressed as functions of temperature by

$$D = D_0 \exp(-E_d/RT) \quad (4)$$

and

$$K = K_0 \exp(-E_s/RT) \quad (5)$$

One may then show the temperature dependence of the permeation process, under conditions of equilibrium at the surfaces, by combining Equations (3), (4), and (5). If in addition p_2 is considered to be negligible compared with p_1 (the usual experimental case), the following expression results:

$$R = \frac{2\pi r_a L D_0 K_0 \exp(-E_p/RT) p_1^{1/2}}{(r_2 - r_1)} \quad (6)$$

where $E_p = E_d + E_s$. Equation (6) is a form of the basic Richardson equation (15).

The Effect of Slow Surface Reactions on Permeation Rates

The principal consequence of slow surface reactions is that the hydrogen atoms dissolved just inside the surface will not be in equilibrium with the hydrogen in contact with the surface (or as nearly in equilibrium as any rate process, such as permeation, will allow). If surface rates are slow, it follows logically that the Richardson equation would not be obeyed. That is the pressure exponent would be different from one-half, and the inverse-thickness and the exponential-temperature relations would not hold.

A detailed analytical treatment of the role surface processes play in gas-metal permeation is given in a recent paper by Ash and Barrer (2). These authors consider the surface processes to be described by six kinetic constants, and couple the resulting surface-rate equations with the diffusion step to produce complicated equations for describing permeation rates.

An approach which yields relatively simple permeation relations, and therefore is of value in treating experimental data, can be made by analogy to the film-resistance techniques of heat transfer.

Consider again radial permeation under isothermal conditions through a thin-wall cylinder of length L , radii r_1

J. R. Phillips is with the California Research Corporation, Richmond, California.

TABLE 1. DIMENSIONS OF PERMEATION MEMBRANES

| Membrane | I.D., (cm.) | $(r_2 - r_1)$, (cm.) | L , (cm.) | r_a , (cm.) | A_a , (sq. cm.) |
|----------|-------------|-----------------------|-------------|---------------|-------------------|
| A | 2.0386 | 0.2475 | 22.86 | 1.143 | 164.2 |
| B | 2.3482 | 0.1011 | 22.86 | 1.225 | 175.9 |
| C | 2.3476 | 0.1003 | 22.86 | 1.224 | 175.8 |
| D | 2.4977 | 0.0252 | 22.86 | 1.262 | 181.2 |

and $r_2 (r_2 > r > r_1)$, and hydrogen pressure p_1 , maintained constant inside, and p_2 , maintained constant outside the cylinder ($p_1 > p_2$). In the steady state c_1 and c_2 will also remain constant with time. Within the metal lattice the rate of diffusion is expressed by Equation (1).

If one ignores whatever actual processes may be taking place at the gas-metal interface, a mass transfer coefficient h_1 may be defined by expressing the rate at the inside surface by

$$R = 2\pi r_1 L h_1 (p_1^{1/2} - c_1/K) \quad (7)$$

where K is the equilibrium constant between the gas phase and gas dissolved in the metal.

Similarly at the outside surface one may write

$$R = 2\pi r_2 L h_2 (c_2/K - p_2^{1/2}) \quad (8)$$

Then by combining Equations (1), (7), and (8) to eliminate c_1 and c_2 , and considering the case where p_2 is negligible compared with p_1 , one obtains the following expression for thin-wall cylinders:

$$R = \frac{2\pi r_a L p_1^{1/2}}{\left[\frac{(r_2 - r_1)}{KD} + \frac{1}{h_1} + \frac{1}{h_2} \right]} \quad (9)$$

In the case where only one of the pressures is varied it is difficult, if not impossible, to distinguish between resistance to gas flow at the entrance and exit surface. It is therefore convenient to define a single interfacial resistance term by

$$\frac{1}{h} = \left(\frac{1}{h_1} + \frac{1}{h_2} \right) \quad (10)$$

Combining Equations (9) and (10) one finds

$$R = \frac{2\pi r_a L p_1^{1/2}}{\left[\frac{(r_2 - r_1)}{KD} + \frac{1}{h} \right]} \quad (11)$$

It is of interest to briefly examine the limiting cases of Equation (11). For the case of very fast surface rates $h = \infty$, and Equation (11) reduces to Equation (3) (with $p_2 = 0$). Thus only when $h = \infty$ is the permeation rate inversely proportional to membrane thickness, and since h may be pressure dependent, only when $h = \infty$

does the square-root-of-pressure relationship hold.

For the case where h is small compared with D Equation (11) reduces to

$$R = 2\pi r_a L h p_1^{1/2} \quad (12)$$

If the permeation rate is limited by resistance at the entrance surface, R may be expected to be directly proportional to p_1 (3, 6). In this case $h = h_1$, and it is implied that h must vary as the square root of pressure.

Membrane Thickness as a Variable

As may be seen from Equation (11) the relative importance of interfacial resistance is in part determined by the value of the thickness. Flint (7) has stated that surface rates should be more controlling with thinner membranes and that under these conditions increased thickness would produce less decrease in permeation rate than predicted by the inverse-thickness relation.

Several investigators (4, 9, 10, 11) have employed the variable-thickness technique as a means of studying the effects of surface rates and apparently verified that the permeation rate is inversely proportional to wall thickness for the systems: hydrogen-nickel, oxygen-silver, and hydrogen-iron.

Raczynski (14) carried out some interesting experiments in which he worked with nascent hydrogen and iron membranes (0.1 to 3.2 mm. thick) in the temperature range of 20° to 90°C. He reported that the permeation rates observed were not proportional to inverse membrane thickness and that excessively low values of permeability were calculated with membranes less than 0.9 mm. thick.

Recently Silberg and Bachman (17), working with molecular hydrogen, studied the rate of permeation of hydrogen through palladium in the temperature range of 200° to 600°C. and at pressures of from 10 to 70 cm. Hg. They found the permeation rate was independent of palladium wall thickness for 5-, 10-, and 20-mil. samples

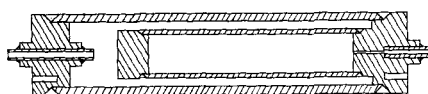


Fig. 1. Permeation assembly.

and state that these data apparently cannot be explained in terms of existing theory. However their data are in agreement with those of Wahlin and Naumann (20) who found that the rate of hydrogen permeation through palladium by electrolysis was independent of changes in wall thickness.

Schenck and Taxhet (16) found that the rate of hydrogen permeation through pure iron and steel was inversely proportional to wall thickness only after fully activating the metal surface.

In summary only three cases are known (14, 17, 20) where hydrogen permeation rates through a metal barrier have been observed to deviate from the inverse-thickness relation in a manner consistent with accepted theory on the effect of slow surface reactions on permeation rates. In only one case (17) was hydrogen gas used.

EXPERIMENTAL

Experimental System

The gas-metal system selected for the experimental phase of the work was hydrogen-AISI type 321 stainless steel, which is a titanium-stabilized austenitic (18-8) stainless, whose general properties are well known (12). Flint (7) has reported the only previously available hydrogen-permeation data on this system.

The permeation membranes were fabricated from commercial aircraft quality, seamless, cold drawn tubing. Before delivery the tubing had been annealed and pickled. The dimensions of the four membranes used are given in Table 1. The compositions, specifications, and complete dimensions and tolerances for each membrane are available (13).

The inside (gas entry surface) of each membrane was mechanically polished to a mirror finish in an attempt to slow the surface reactions as much as possible and to localize any observed interfacial resistance at the entrance surface.

Two sources of hydrogen were used in these experiments. For the low-pressure runs (10 atm. and below) a cylinder of low-oxygen-content hydrogen (oxygen and water content of 10 parts/million each) was used. A cylinder of dry hydrogen (oxygen content 3 to 5 parts/million, water content 1.3 parts/million) was used for the 30-atm. runs.

An oxygen and water removal train was included as part of the gas-delivery system. Hydrogen leaving the former cylinder passed through a deoxidation unit where any oxygen present in the hydrogen was catalytically converted to water. The unit used specified a maximum flow capacity of 25 SCHF, maximum operating pressure of 2,500 lb./sq.in. gauge, and maximum entrance oxygen content of 3% in order to obtain less than 1 part/million oxygen in the exit hydrogen. In practice hydrogen was delivered at low (but unmeasured) flow rates with an oxygen content of about 10 parts/million. To remove water from the hydrogen it next passed through a

1¼ in. diameter by 5¼ in. length bed containing 6 to 16-mesh silica gel and then through an identical bed filled with type 5-A, 1/16 in. pellet molecular sieves. It is believed that hydrogen leaving the latter bed contained a concentration of no greater than 1 part/million oxygen or water.

The dry hydrogen bypassed the de-oxidation unit and silica-gel bed but did go through the molecular sieve bed. This fact is not serious, as the dry hydrogen had initially low oxygen and water contents and was used for only a limited number of runs.

Experimental Method and Apparatus

The basic experimental technique employed to measure permeation rates was standard and has been used many times in the past (3, 5, 8). It consisted of maintaining a constant hydrogen pressure p_1 on the inside of the permeation membrane, while the exit surface was kept under a high vacuum. Initially the hydrogen was charged as a pulse at p_1 to the previously degassed metal membrane. The permeation rate then went through an unsteady state as the hydrogen concentration gradient developed within the metal until the steady state was achieved. The rate of permeation was determined by measuring the rate of pressure rise in a known volume which was in contact with the exit surface of the permeation membrane. The temperature of the gas in the collecting system was measured, and thus the rate of gas permeation was readily calculated with the ideal gas law.

The variables studied were hydrogen pressure at the entrance surface of the permeation membrane (0.1 to 30.0 atm.), temperature of the permeation membrane (300° to 800°C.), and membrane wall thickness (0.0252 to 0.2475 cm.).

The experimental apparatus consisted of four major components. The basic purpose and function of each component will be briefly described below.

The permeation assembly. The permeation assembly allowed high-pressure hydrogen to be maintained on one side of a metal membrane and a high vacuum to be maintained on the other side while the assembly was at a high temperature.

The entire permeation assembly was made of type 321 stainless steel. Four permeation assemblies were made, all identical, except for the variable wall thickness of the permeation membranes and some slight modifications required for the thinnest-walled membrane. The assemblies were fabricated in accordance with Figure 1. In an experiment hydrogen was charged to the inside of the membrane and permeated radially out into the surrounding evacuated space. Both the delivery and vacuum lead tubes were about 15 in. long, which enabled connections to be made to the delivery and collecting systems outside the furnace. Holes for thermocouples are indicated in each end plug, and additional thermocouples were located in tubes welded to the side of the assembly.

As may be seen from Figure 1 it was necessary to seal the assembly in several places. The seals were accomplished by heliarc welding, and each was tested with

TABLE 2. PRESSURE EXPONENT AS A FUNCTION OF TEMPERATURE, PRESSURE AND THICKNESS

| Membrane A: ($r_2 - r_1$) = 0.2475 cm. | | | | |
|---|------------------|------|------|-------|
| Temperature, (°C.) | Pressure, (atm.) | | | |
| | 0.1 | 1.0 | 10.0 | |
| 600 and 400 | 0.55 | 0.55 | 0.54 | |
| Membrane B: ($r_2 - r_1$) = 0.1011 cm. | | | | |
| Temperature, (°C.) | Pressure, (atm.) | | | |
| | 0.1 | 1.0 | 10.0 | 30.0 |
| 800 | 0.55 | 0.55 | | |
| 600 and 400 | 0.63 | 0.59 | 0.55 | 0.55* |
| 300 | 0.59 | 0.55 | 0.50 | |
| Membrane D†: ($r_2 - r_1$) = 0.0252 cm. | | | | |
| Temperature, (°C.) | Pressure, (atm.) | | | |
| | 0.1 and 1.0 | | | |
| 600 | ~0.83 | | | |
| 400 | ~1.0 | | | |

* 400°C. only.

† It was impossible to establish quantitatively the effect of pressure and temperature on the permeation rates through membrane D, owing to the great effect of interfacial resistance encountered and the resulting change of permeation rates with time. This latter phenomenon is discussed later.

a helium leak detector to insure that it was tight.

For purposes of treating the data it has been assumed that the end plugs of the permeation membranes were perfect insulators. This assumption is not strictly true, but calculations show that the amount of gas flowing through the plugs will be on the order of 1% of the total in the worst case.

Gas-delivery system. A leak-tight, gas delivery system was required such that a constant hydrogen pressure might be maintained on the permeation membrane for extended periods of time (over 24 hr.). The system was capable of delivering hydrogen at both relatively high (30 atm.) and relatively low (0.10 atm.) pressures.

Accurate pressure measurements were of prime importance in this work. To measure pressure for the 1 atm. runs an open-end mercury manometer was used in conjunction with a nearby barometer. A 500 lb./sq. in. gauge was used to determine pressures for the 10- and 30-atm. runs. For the 0.1-atm. runs the pressure was measured with a closed-end mercury U-tube.

Gas-collecting system. A leak-tight vacuum system was needed to collect and measure the amount of hydrogen which had passed through the permeation membrane. At the same time a negligible back pressure had to be maintained on the exit surface of the membrane throughout the course of an experimental run. This was accomplished with a mercury diffusion pump which divided the collecting system into two parts. The permeated gas was pumped away from the membrane, through the dynamic section, and then collected in the static section. A vacuum gauge was used to insure that the pressure remained negligible behind the diffusion pump (that is at the exit surface of the membrane).

The static section (essentially a constant volume section) contained two large glass bulbs with stopcocks as collecting volumes. Pressure in the section was measured with a slightly modified three-scale McLeod type of vacuum gauge. A gas sampling bulb could be introduced into the section through a ground glass joint provided.

Temperature measurement and control. An electric-resistance type of furnace that could achieve and maintain high temperatures (up to 800°C.) for periods of several days was used. The temperature was measured with four thermocouples and controlled manually with a variable transformer.

In addition equipment was provided for maintaining an argon blanket in the furnace around the permeation assembly whenever the assembly was above room temperature.

Degassing and Blank Accumulation

Prior to the use of a membrane it was degassed, with a vacuum maintained on both sides, at high temperature (800°C. for A, B, and C and 600°C. for D) for at least 21 hr. This served both to remove residual gases dissolved in the metal and to insure complete annealing of the membrane.

At elevated temperatures gas accumulated in the collecting system even when the hydrogen pressure was zero on the high side of the membrane. This phenomenon was termed *blank accumulation*. A minimum blank accumulation rate was observed for each membrane at a given temperature. These rates were small when compared with the total rate at which gas was collected during a permeation run (less than 1% in the majority of cases and less than 10% in the case of the slowest permeation rates observed) and somewhat reproducible from assembly to assembly.

The nature and origin of the gas collected as a result of blank accumulation are open to speculation. There are two main possibilities: either these foreign gases resulted from incomplete degassing of the permeation assembly, or they somehow permeated into the collecting system from outside the assembly. As the result of an accumulation of experience (5, 8, 13) with this phenomenon the latter explanation is believed correct.

ANALYSIS OF RESULTS

Calculation Procedure

A procedure was developed for the IBM-650 data processing system by which the basic quantities of interest in gas-metal permeation work (for example the permeation rate) could be determined from the raw experimental data of a given run. The program was originally written in Fortran language, and the final form of the Fortran listing, as well as a complete description of the program, is available (13). In general if the basic experimental method used in this work is followed, this program may be used for the resulting permeation calculations.

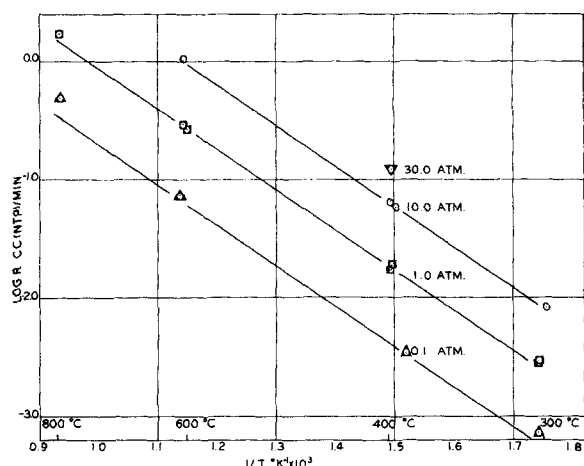


Fig. 2. Log of permeation rate vs. reciprocal of absolute temperature, membrane B.

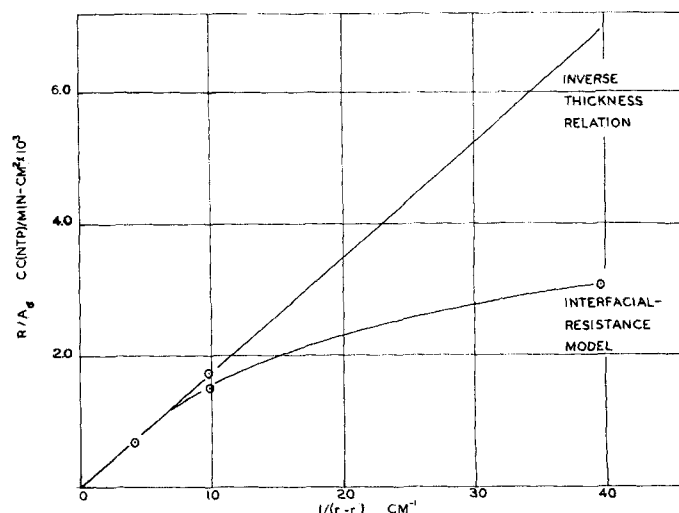


Fig. 3. Permeation rate vs. inverse membrane thickness at 1.0 atm. and 608.3°C.

Experimental Data

Temperature. The effect of temperature on the permeation rates through each membrane was determined by plotting the log of the permeation rates vs. the reciprocal of absolute temperature, as in Figure 2 for membrane B.

Figure 2 shows that an Arrhenius type of plot of the data does not yield a true straight line but that a slight curvature results. The curvature becomes more pronounced at lower pressures, and in order to obtain a meaningful value for the activation energy only the data at 1 atm. and above were considered.

Deviation from the exponential-temperature relation, similar to that observed here, was reported by Flint (7) who worked with the system: hydrogen type 347 stainless steel. Also the solubility data of Armbruster (1) show a slight curvature when plotted this way.

The resulting activation energies of permeation E_p are given in Table 3. Activation energies found with the thicker membranes (A, B, and C) were nearly the same and close to that found by Flint (7). However the activation energy found with the thinnest membrane, although not well established quantitatively, was significantly greater than that of the others. An explanation of this can be seen by reference to Equation (11). If, with the thinnest membrane, the interfacial resistance $1/h$ becomes important, and the interfacial mass transfer coefficient h has an activation energy different from $(E_d + E_s)$, then the total temperature effect will be influenced, at least in part, by h , resulting in the observed increase of E_p noted with membrane D.

Pressure. The method used to establish the pressure exponent was simply to compare the permeation rates at various pressures with the rate at 1 atm. for a given temperature. Using the empirical relation

$$\frac{R_p}{R_{1.0}} = p^n \quad (13)$$

one may readily calculate n . The value of n at 1.0 atm. was taken as the arithmetic average of n from 0.1 to 1.0 atm. and from 1.0 to 10.0 atm.

Values of the pressure exponent n determined in this manner are given in Table 2. It should be pointed out that the values of n reported in this table are not point values of n at the pressure in question. They represent an average pressure effect over at least a tenfold pressure range. True point values of n at 0.1 atm. would be greater than those reported, and point values of n at 10.0 atm. and above would be closer to $1/2$ than those reported.

In many cases values of n significantly greater than $1/2$ were found. In general the trend was toward higher values of n at lower temperatures, with a definite trend toward higher values of n at lower pressures. In addition values of n became greater as the membrane thickness decreased, other variables being held constant. These observations are consistent with the observation by Chang and Bennett (6) that when surface reactions are important, it is to be expected that n will more closely approach unity the lower the pressure and temperature.

Thickness. The most interesting and valuable results of this work were gained by the use of membrane thickness as a variable. The Richardson equation implies that the permeation rate is inversely proportional to the membrane thickness. However the results of the present work indicate that under the proper conditions the permeation rate tends to become independent of the membrane wall thickness for the hydrogen type 321 stainless steel system.

In Figure 3 the total permeation rate divided by the area available for per-

meation is plotted as a function of inverse wall thickness for a typical set of conditions. The area term is included to compensate for the fact that the area available for permeation was not exactly the same for each membrane. The point nearest the origin represents A (the thickest permeation membrane), the next two points represent B and C, and the final point represents D (the thinnest permeation membrane). Included in this figure is a straight line which represents rates predicted by the inverse-thickness relation, with the thickest membrane as a basis. Also included in Figure 3 is a curve, representing the interfacial-resistance model calculated from Equation (11), with constants presented in Table 4.

The behavior indicated in Figure 3 was typical of that observed under other conditions of temperature and pressure where it was possible to obtain permeation-rate data over the entire range of membrane thickness. The rates observed for the thinnest membrane were much less than those predicted by the inverse-thickness relation. In fact even with the intermediate-thickness membrane C the rates tended to be lower than those predicted by the inverse-thickness relation. The trend of the experimental data indicates that the rates tend to become independent of wall thickness for very thin walls (which corresponds to the case where the permeation rates are completely controlled by surface reactions).

Correlation of Results

Permeability. The most common way to correlate permeation-rate data is in terms of the permeability. In order to do this one must assume that the Richardson equation [Equation (6)] is applicable and then reduce the permeation-rate data to a set of standard conditions. The conditions normally adopted for reporting the permeability

are 1-atm. pressure, 1-mm. metal thickness, and 1 sq. cm. of permeation area. Since by definition

$$P = \frac{R(r_2 - r_1)}{A_0 p_1^{1/2}} \quad (14)$$

one may rewrite Equation (6) in the form of a permeability expression as

$$P = P_0 \exp(-E_p/RT) \quad (15)$$

where $P_0 \equiv D_0 K_0$. Equation (15) is analogous to Equation (6), but important differences exist which must be clearly in mind.

If the Richardson equation applied to the system in question, the activation energy and the factor P_0 would be constant in all five cases reported in Table 3. The fact is that although the permeability expressions calculated for the two thicker membranes A and B are nearly the same, in general the permeability expressions obtained in this work are dependent on membrane thickness. Values of the permeability at a given temperature tend to become lower as the membrane thickness decreases.

The values of permeability determined here were in all cases lower than the values of the permeability for the system calculated from the data of Flint (7). This is probably due to the highly polished membrane surfaces employed in the present work, which slowed the observed permeation rates.

The prediction of permeation rates from values of permeability reported in the literature may result in large errors. For example under the conditions of 604°C. and 0.1 atm. the permeability expression based on membrane A predicts a rate of 38.4×10^{-2} cc. (NTP)/min. for membrane D. The observed permeation rate for membrane D under these conditions was 9.91×10^{-2} cc. (NTP)/min., or the predicted rate is high by a factor of nearly 4. In order to correctly describe the permeation behavior of a hydrogen-metal system the membrane thickness limits as well as the temperature and pressure limits of a proposed expression must be stated.

For membranes thicker than 0.2475 cm., temperature between 300° and

TABLE 4. CONSTANTS FOR INTERFACIAL-RESISTANCE MODEL

| Temperature, (°C.) | Pressure, (atm.) | h , [$\frac{\text{cc. (NTP)}}{\text{min. (atm.)}^{1/2} \text{ sq. cm.}}$] | D , [$\frac{\text{sq. cm.}}{\text{sec.}}$] | K , [$\frac{\text{cc. (NTP)}}{\text{cc. (atm.)}^{1/2}}$] |
|-----------------------|---------------------|--|---|---|
| 608.3 | 1.0 | 46.8×10^{-4} | 10.2×10^{-6} | 3.81×10^{-1} |
| 604.0 | 0.1 | 22.6×10^{-4} | 10.0×10^{-6} | 3.78×10^{-1} |
| 401.4 | 1.0 | 1.38×10^{-4} | 1.11×10^{-6} | 2.60×10^{-1} |

800°C., and pressure greater than 0.1 atm. the following permeability expression may be used to predict permeation rates for the hydrogen type 321 stainless steel system:

$$P = 14.2 \exp(-15,700/RT) \quad (16)$$

Interfacial-Resistance Model. In order to use Equation (11) to correlate experimental permeation data two constants (h and the product KD) must be evaluated. A basic assumption in the determination of values of h from a quantitative treatment of the thickness effect is that the interfacial resistance is constant from membrane to membrane under the same conditions of temperature and pressure. It is probable that this condition was not entirely satisfied in this work, and values of h (and the product KD) should be considered as order-of-magnitude estimates.

Constants evaluated for use with Equation (11) are given in Table 4. The product KD was split into its components with Armbruster's (1) values for the solubility. The constants are presented for three sets of temperature-pressure conditions, for which data are available for all four permeation membranes studied.

By means of the constants presented in Table 4 a plot of Equation (11) has been made in Figure 3 for the conditions of 1.0 atm. and 608.3°C. The model fits the data of Figure 3 within 11% for the worst case. Similarly the model fits the data obtained at 0.1 atm. and 604.0°C. within 12% and the data obtained at 1.0 atm. and 401.4°C. within 34%. In the latter case use of the inverse-thickness relation leads to errors greater than 300%.

Table 4 brings out the fact that the value of the interfacial mass transfer coefficient h is both pressure and tem-

perature dependent. Thus a decrease in pressure or temperature tends to decrease the value of h and consequently increases the absolute value of the interfacial resistance as represented by $1/h$.

Reproducibility

Reproducibility of data was studied extensively with membrane B through three heating and cooling cycles and over the course of twenty experimental runs. There was a tendency for the rates to increase if several experiments were made in between runs repeated under otherwise identical conditions. For membrane B the total increase amounted to about 6% on the average, with a maximum of 13%.

For the other membranes the observed increases were more pronounced but were confined to the first few runs or the first hours of exposure of the membrane to hydrogen. The most pronounced effect was encountered with membrane A. Here the observed rate increased by a factor of nearly 3 during the course of the first six runs (or during the first 17 hr. the membrane was exposed to hydrogen). Thereafter the rate remained constant.

It is pointed out that the data which were correlated and interpreted in the preceding sections were either the results from experiments made during a time interval when there was little, if any, change of rates with time (that is after an initial period in which the rates were observed to increase had passed), or the highest rates observed (under a given set of conditions).

In order to learn the cause of the observed increase of permeation rates with time membrane B was inspected upon completion of the desired permeation experiments. The outside, or exit, surface appeared to undergo little, if any, change as a result of the experiments. However the inside, or gas entry, surface was found to be covered with a finely divided black powder. An x-ray analysis (19) of the black powder indicated that it was primarily stainless steel in some finely divided form. A microscopic examination (19) of the internal structure of the membrane revealed no apparent structure change in the metal due to the hydrogen permeation experiments.

In light of these findings it is postulated that the phenomenon of permea-

TABLE 3. PERMEABILITY OF HYDROGEN TYPE 321 STAINLESS STEEL SYSTEM

Constants for $P = P_0 \exp(-E_p/RT)$

| Source | $r_1 - r_2$, (cm.) | $\left(\frac{E_p, \text{ cal.}}{\text{g. mole}}\right)$ | $\left[\frac{P_0, \text{ cc. (NTP)}}{\text{min. sq. cm.}} \left(\frac{\text{mm.}}{\text{atm.}^{1/2}}\right)\right]$ | P , (at 600°C.) |
|------------|---------------------|---|---|-----------------------|
| Membrane A | 0.2475 | 15,740 | 14.20 | 1.63×10^{-3} |
| Membrane B | 0.1011 | 15,650 | 13.95 | 1.69×10^{-3} |
| Membrane C | 0.1003 | 15,650 | 12.10 | 1.46×10^{-3} |
| Membrane D | 0.0252 | 20,150 | 77.50 | 0.70×10^{-3} |
| Flint (7) | 0.0864 | 15,500 | 16.50 | 2.17×10^{-3} |

tion rates changing with time of membrane exposure to hydrogen was due to a surface effect. In fact the increase of permeation rates observed under identical conditions of pressure and temperature can be considered to be the result of an increase in surface activity.

These results, inadvertently obtained here, showing that the permeation rates changed with time, support the evidence that surface reactions exert a great influence on permeation rates in the hydrogen type 321 stainless steel system. However they tended to hinder quantitative treatment of the data. For example the proposed permeability expression should be considered valid only after any initial activation of the membrane surface has taken place.

ACKNOWLEDGMENT

The authors wish to express their appreciation to Dr. Raymond W. Southworth, Chemical Engineering Department, Yale University, for writing the program for the IBM-650 data processing system which was used in this study.

The authors also wish to express their gratitude for financial aid in support of this work from the Higgins Fund, administered by Yale University, and from the American Viscose Corporation.

NOTATION

- A = area, permeation area, area perpendicular to the direction of gas flow, sq. cm.
 A_a = arithmetic average permeation area for a hollow cylinder, sq. cm.
 c = concentration (atomic) of gas within the metal lattice, cc. (NTP)/cc.*
 D = diffusivity or diffusion coefficient, sq. cm./sec., or sq. cm./min.
 D_0 = value of D at infinite temperature, frequency factor, sq. cm./min.

- E_d = activation energy for diffusion, cal./g. mole
 E_p = activation energy for the permeation process, cal./g. mole
 E_s = activation energy for solubility or heat of solution, cal./g. mole
 h = mass transfer coefficient for interfacial-resistance model, cc.(NTP)/sq. cm. min.(atm.)^{1/2}*
 K = solubility constant, cc.(NTP)/cc.(atm.)^{1/2}
 K_0 = solubility constant at infinite temperature, cc.(NTP)/cc.(atm.)^{1/2}
 L = length of permeation membrane, cm.
 n = pressure exponent, $1/2 < n < 1$
 P = permeability, $\left[\frac{\text{cc. (NTP)}}{\text{sq. cm. min.}} \right] \left(\frac{\text{mm.}}{(\text{atm.})^{1/2}} \right)$
 P_0 = permeability at infinite temperature, $\left[\frac{\text{cc. (NTP)}}{\text{sq. cm. min.}} \right] \left(\frac{\text{mm.}}{(\text{atm.})^{1/2}} \right)$
 p = gas pressure, atm.*
 R = rate of permeation, total rate of gas permeation or diffusion through a metal barrier, cc. (NTP)/min.
 R = molar gas constant, 1.987 cal./g. mole (°K.)
 r = radial distance in a cylinder, cm.*
 r_a = arithmetic average radius, equal to r_m for thin-walled cylinders, cm.
 r_m = log mean radius, $(r_2 - r_1)/\ln r_2/r_1$, cm.
 T = absolute temperature, °K.

* Subscripts 1 and 2 refer to conditions at the entrance and exit surfaces, respectively, for p , c , r , and h .

LITERATURE CITED

- Armbruster, M. H., *J. Am. Chem. Soc.*, **65**, 1043 (1943).
- Ash, R., and R. M. Barrer, *Phil. Mag.*, **47**, 1197 (1959).
- Barrer, R. M., "Diffusion in and through Solids," Cambridge University Press, Cambridge, England (1951).
- Baukloh, W., and H. Kayser, *Z. Metallk.*, **26**, 156 (1934).
- Bryan, W. C., D. Eng. dissertation, Yale Univ., New Haven, Connecticut (1959).
- Chang, P. L., and W. D. G. Bennett, *J. Iron and Steel Inst.*, **170**, 208 (1952).
- Flint, P. S., Knoll's Atomic Power Laboratory, Schenectady, New York, *KAPL-659* (December 14, 1951).
- Harden, K. L., M. Eng. thesis, Yale Univ., New Haven, Connecticut (1957).
- Johnson, F. M. G., and P. Larose, *J. Am. Chem. Soc.*, **46**, 1377 (1924).
- Lewkonja, G., and W. Baukloh, *Z. Metallk.*, **25**, 399 (1933).
- Lombard, V. M., *Compt. rend.*, **177**, 116 (1923).
- "Metals Handbook," Am. Soc. for Metals, Cleveland, Ohio (1948).
- Phillips, J. R., D. Eng. dissertation, Yale Univ., New Haven, Connecticut (1960).
- Raczynski, W., *Arch. Hutnictwa*, **3**, 59 (1958). (See *Chem. Abs.*, **52**, 15205.)
- Richardson, O. W., *Phil. Mag.*, **7**, 266 (1904); **8**, 1 (1904).
- Schenk, H., and H. Taxhet, *Arch. Eisenhüttenw.*, **30**, 661 (1959).
- Silberg, P. A., and C. H. Bachman, *J. Chem. Phys.*, **29**, 777 (1958).
- Sims, C. E., "Gases in Metals," pp. 119-198, Am. Soc. for Metals, Cleveland, Ohio (1953).
- Tetelman, A. S., Private communication, Yale Univ., New Haven, Connecticut (December 29, 1959).
- Wahlin, H. B., and V. O. Naumann, *J. Appl. Phys.*, **24**, 42 (1953).

Manuscript received October 13, 1961; revision received June 29, 1962; paper accepted July 2, 1962. Paper presented at A.I.Ch.E. Los Angeles meeting.

Behavior of Non-Newtonian Fluids in the Inlet Region of a Channel

MORTON COLLINS and W. R. SCHOWALTER

Princeton University, Princeton, New Jersey

Under the impetus of both academic curiosity and practical necessity considerable effort has been expended in recent years toward finding solutions to the differential equation of motion

for non-Newtonian fluids. As one might expect exact solutions are available only for relatively simple geometries and rheological equations of state (the set of equations relating the state of stress of the fluid under consideration to its velocity field). For a discussion

dealing with some of the problems inherent in obtaining solutions to the equation of motion the reader is referred to a review by Oldroyd (7).

It has become evident that approximate solutions to the equation of motion can be of value for non-Newtonian

Morton Collins is with the Esso Research and Engineering Company, Linden, New Jersey.